

Electronic Supplementary Information (ESI) for

**Heterogeneously Ni–Pd nanoparticle-catalyzed base-free formal C–S
bond metathesis of thiols**

Kanju Mitamura,^a Takafumi Yatabe,^{*a} Kidai Yamamoto,^a Tomohiro Yabe,^a

Kosuke Suzuki,^a and Kazuya Yamaguchi^{*a}

^aDepartment of Applied Chemistry, School of Engineering, The University of Tokyo, 7-3-1 Hongo, Bunkyo-ku, Tokyo 113-8656, Japan

**e-mail: kyama@appchem.t.u-tokyo.ac.jp, yatabe@appchem.t.u-tokyo.ac.jp*

Table of Contents

Experimental	S2–S4
Additional Notes	S5–S6
Supplementary Figures	S7–S10
Supplementary Tables	S11–S15
Spectral Data	S16–S19
Supplementary References	S20
NMR Spectra	S21–S29

Experimental

Instruments and Regents

Gas Chromatography (GC) analyses were performed on Shimadzu GC2014 equipped with a flame ionization detector (FID) and capillary columns (InertCap5) using Shimadzu C-R8A Chromatopac Data Processor for area calculations. GC mass spectrometry (GC-MS) spectra were recorded on Shimadzu GCMS-QP2010 or GCMS-QP2020 equipped with an InertCap5 capillary column at an ionization voltage of 70 eV. Liquid-state NMR spectra were recorded on JEOL JNM-ECA-500. ^1H and ^{13}C NMR spectra were measured at 500.2 and 125.8 MHz, respectively, using tetramethylsilane (TMS) as an internal standard ($\delta = 0$ ppm). ICP-AES analyses were performed on Shimadzu ICPS-8100. Scanning transmission electron microscopy (STEM) observations were performed on a JEOL JEM-ARM200F. XRD patterns were recorded using a Rigaku SmartLab instrument under $\text{Cu K}\alpha$ radiation (45 kV, 200 mA). BET surface areas were measured on micromeritics ASAP 2010 and calculated from the N_2 adsorption isotherm with the BET equation. Pd K-edge X-ray absorption spectroscopy (XAS) was carried out at the BL14B2 beamline of SPring-8 (Proposal No. 2019B1820) and Ni K-edge XAS was carried out at the BL11S2 beamline of the Aichi Synchrotron Radiation Center, Aichi Science & Technology Foundation (Proposal No. 201905093). XAS measurements were conducted in transmission mode using both Si (111) and Si (311) crystal monochromators. Each sample was formed into a pellet, doubly wrapped in an Al laminate pack, and heat-sealed in an Ar-filled glovebox. X-ray absorption near-edge structure (XANES) and extended X-ray absorption fine structure (EXAFS) data were analyzed using Athena and Artemis software (Demeter, ver. 0.9.025; Bruce Ravel). The k^3 -weighed EXAFS spectra were Fourier-transformed into R -space at 3.0–12.0 \AA^{-1} . The back Fourier-transform obtained in the R range of 1.0–3.2 \AA was used for curve-fitting. Pd foil was used as standard samples. IFFEFIT (Athena and Artemis) programs were used for data analysis, treatment, and modeling. FEFF6 was used to generate Feff.inp files for analysis by Artemis using the atomic coordinates of the relevant theoretical references calculated using X-ray crystallographic methods available in the literature^{S1}: Ni and Pd. The structure of the scattered atoms (Pd) around the absorbing atoms (Ni) was created by FEFF6 using the atomic coordinates of the relevant theoretical references of Ni and Pd, respectively, and phase shifts and backscattering amplitude of Ni–Pd were calculated. Column chromatography on silica gel was performed by using Biotage Isolera. $\text{Ca}_{10}(\text{PO}_4)_6(\text{OH})_2$ (HAP, BET surface area: 11 m^2g^{-1} , 011-14882, Wako), CeO_2 (BET surface area: 92 m^2g^{-1} , JRC-CEO-5, Daiichi Kigenso Kagaku Kogyo), Al_2O_3 (BET surface area: 160 m^2g^{-1} after calcination at 550 $^\circ\text{C}$ for 3 h, KHS-24, Sumitomo Chemical), TiO_2 (BET surface area: 316 m^2g^{-1} , ST-01, Ishihara Sangyo Kaisya), $\text{Mg}_6\text{Al}_2(\text{OH})_{16}\text{CO}_3 \cdot 4\text{H}_2\text{O}$ (LDH, BET surface area: 51 m^2g^{-1} , Tomita Pharmaceutical Co., Ltd.), were commercially available. Solvents, substrates, and metal sources were obtained from TCI, Aldrich, Kanto Chemical, FUJIFILM Wako Pure Chemical, Nacalai Tesque, Kojima Chemicals, or Combi-Blocks (reagent grade), and purified prior to the use, if necessary.

Preparation of Supported Ni–Pd Catalysts

Ni–Pd/HAP was prepared as follows. First, HAP (2.0 g) was added to a 100 mL aqueous solution of NiCl₂·6H₂O (4.0 mM) and K₂PdCl₄ (4.0 mM) which was generated *in situ* from a mixture of PdCl₂ (0.4 mmol) and KCl (0.8 mmol). After stirring 15 min, 1M NaOH aq. was added dropwise to adjust pH = 11.5. The resulting slurry was stirred for 24 h at room temperature. The solid was filtered off, washed with water (3 L), and dried in *vacuo* overnight to afford a hydroxide precursor (brownish yellow powder). 1.0 g of the hydroxide precursor was dispersed in 25 mL degassed water and reduced by NaBH₄ (120 mg) at room temperature for 2 h under an Ar atmosphere. The solid was once again filtered off, washed with ethanol (75 mL), and dried in *vacuo* 3 h to afford Ni–Pd/HAP catalyst (gray powder, Ni: 0.98wt%, Pd: 1.92wt% determined by ICP-AES). Other supported metal catalysts were prepared by the similar methods. CoCl₂·6H₂O, FeCl₃·6H₂O, RuCl₃, RhCl₃, H₂Pt(OH)₆ and CuCl₂·2H₂O was used as Co, Fe, Ru, Rh, Pt and Cu precursor, respectively. In the case of supporting Pt, the adjusted pH was 7.5 using NaOH and HNO₃.

Catalytic Reaction

The catalytic reaction was typically carried out according to the following procedure. Into a glass Schlenk tube (volume: approximately 20 mL) were added Ni–Pd/HAP (100 mg, Ni: 4.0 mol%, Pd: 4.0 mol%), and a Teflon-coated magnetic stir bar under an Ar atmosphere; into another glass Schlenk tube were successively added biphenyl (0.1mmol, internal standard), *p*-toluene thiol (**1a**, 0.5 mmol), and mesitylene (2 mL); Through freeze-pump-thaw cycling, the dissolved gases were removed from the solution, and the atmosphere was replaced into an Ar atmosphere; this solution was added into the Schlenk tube containing the catalyst by syringe, and the atmosphere was replaced into an H₂ atmosphere; the mixture was then stirred at 150 °C for 24 h with an H₂ balloon. The yields of products were determined by GC analysis using biphenyl as an internal standard. The products were identified by GC-MS and NMR.

Isolation of Products

Typical procedures for isolation of desired thioether products are as follows. After the reaction was finished, the catalyst was filtered off and the filtrate was added to (C₂H₅)₂O (10 mL). Next, to remove remaining thiols, the solution was washed with 1M NaOH aq. (10 mL), extracted by (C₂H₅)₂O (3×10 mL), and then evaporated to remove solvents. The crude product was subjected to silica-gel column chromatography using hexane as the eluent, giving the pure product.

Hot Filtration

The catalyst was removed by hot filtration under an N₂ atmosphere 4 h after the reaction started under the optimized conditions using an H₂ balloon, and the reaction was again carried out with the filtrate

under the same conditions. When the amount of leached metals was measured, the filtrate after the reaction for 24 h was evaporated *in vacuo*, treated with concentrated aqua regia (1 mL), and sonicated. Then, Ni and Pd species in the filtrate were analyzed by ICP-AES after the filtrate was moved into a 10 mL volumetric flask.

Reuse Test

The reuse of catalyst was carried out as follows. After the reaction, Ni–Pd/HAP was filtered off and washed with acetone (100 mL). The used Ni–Pd/HAP was calcinated at 300 °C for 2 h under an air atmosphere. The calcinated Ni–Pd/HAP (200 mg) was dispersed in 25 mL water and reduced with NaBH₄ (120 mg) under an Ar atmosphere. The resulting slurry was then stirred vigorously at room temperature for 2 h. The solid was then filtered off, washed with EtOH (75 mL), and dried *in vacuo* for 3 h, giving the regenerated catalyst as a dark-gray powder.

Cross-Coupling of 1a with a Grignard Reagent

Experiments of Grignard reagent used as nucleophile instead of *p*-toluene thiol were carried out as follows. Into a glass Schlenk tube were added the catalyst and a Teflon-coated magnetic stir bar under an Ar atmosphere; into another glass Schlenk tube were successively added *n*-hexadecane (0.1 mmol) as an internal standard, *p*-toluene thiol (**1a**, 0.5 mmol), and mesitylene solvent; Through freeze-pump-thaw cycling, the dissolved gases were removed from the solution, and the atmosphere was replaced into an Ar atmosphere; this solution was added into the Schlenk tube containing the catalyst by syringe, and 1.35 mL PhMgBr solution in THF (1.1 M, 3 eq.) was added by syringe. The mixture was then stirred at 150 °C for 24 h with an Ar balloon.

Additional Notes

Detailed Discussion of Ni–Pd Bimetallic Structures on HAP

As shown in Fig. 2h, the XRD pattern of Ni–Pd/HAP under an Ar atmosphere showed no peaks derived from Ni or Pd species. Thus, the presence of Ni and/or Pd-derived bulk structures is not under consideration. To think about the phase composition of the Ni–Pd species supported on HAP in the nanoscale, the details of respective metal species can be discussed with the XAFS spectra to some extent. As shown in Fig. 2b, the Pd K-edge XANES spectrum of Ni–Pd/HAP was similar to that of the Pd foil, indicating the Pd valence of zero. The curve fitting analysis of the Pd K-edge EXAFS spectrum of Ni–Pd/HAP suggested the presence of both Ni–Pd bond and Pd–Pd bond (Fig. S2, Table S1, ESI†). Moreover, the coordination number of Pd–Pd bond (C.N. = 5.3) is much larger than that of Ni–Pd bond (C.N. = 1.6), and the Ni/Pd molar ratio = ~1/1 in the Ni–Pd/HAP catalyst is determined using ICP-AES, indicating the presence of monometallic Pd(0) species without being alloyed. On the other hand, the Ni K-edge XANES spectrum of Ni–Pd/HAP was between those of Ni foil and Ni(OH)₂ as shown in Fig. 2a; linear combination fitting (LCF) revealed that ~54% of the Ni species in Ni–Pd/HAP was present at zero valence (Fig. S1, ESI†). In other words, ~46% of the Ni species was present as Ni(II) species. This LCF result is consistent with the presence of monometallic Pd(0) species suggested by the Pd K-edge EXAFS. In addition, considering the fact that the coordination number of Ni–Pd bond is considerably smaller than that of Pd–Pd bond in the Pd K-edge EXAFS spectrum, it is possible that a part of Ni(0) species is present as a monometallic Ni(0) species. Considering these results, in the Ni–Pd/HAP catalyst, Ni–Pd alloy species, Ni(0) species, Ni(II) oxide/hydroxide species, and Pd(0) species are possibly present. Although it is quite difficult to determine the composition of these species, Ni(II) oxide/hydroxide species are probably supported directly on HAP without being reduced by NaBH₄. Also, Ni(0) species cannot be formed without Pd species according to the Ni K-edge XANES spectra of Ni/HAP (Fig. S3, ESI†), suggesting that the Ni(0) species in Ni–Pd/HAP is near the Ni–Pd alloy species and/or Pd(0) species. In addition, given the fact that the binary alloy phase system of Ni and Pd is all proportional solid solution and that NaBH₄ in water is a strong reductant, we assume that main compositions of Ni–Pd alloy species, Ni(0) species, and Pd(0) species on HAP are likely Ni(0) nanoparticles possessing a part of Ni–Pd alloy species, Pd(0) nanoparticles possessing a part of Ni–Pd alloy species, and monometallic Pd(0) nanoparticles, respectively. However, further investigation is necessary to determine the composition clearly.

Physical Mixture of Ni/HAP and Pd/HAP under an H₂ Atmosphere

The physical mixture of Ni/HAP and Pd/HAP under an H₂ atmosphere afforded **2a** in a high yield (Table S4, entry 3). Under the reaction conditions, about 16% of Ni species in the physical mixture catalyst leached into the reaction solution at the short time point, and almost no leaching species were detected at the long time point, while such leaching phenomena were hardly observed in the case of

Ni–Pd/HAP (Table S5). Sakurai *et al.* reported that Au/Pd bimetallic nanoparticles were *in-situ* generated through interaction of Au nanoparticles with leached Pd species in the presence of reductants.^{S2} Moreover, under an Ar atmosphere, the physical mixture of Ni/HAP and Pd/HAP showed a lower catalytic activity than that of Ni–Pd/HAP (Table 1, entries 5 and 6). Considering these results and the previous report, we assume that *in-situ* formed Ni–Pd nanoparticles derived from interaction of supported Pd nanoparticles with leached Ni species in the reaction system was likely active species when the physical mixture catalyst was used under an H₂ atmosphere.

Reuse Test of Ni–Pd/HAP

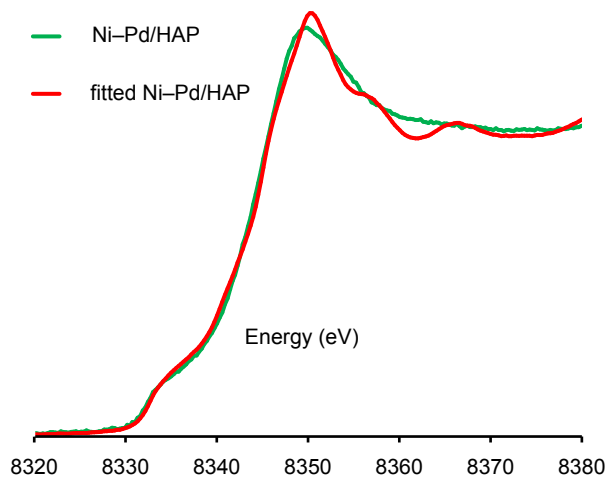
Ni–Pd/HAP recovered after the reaction of **1a** was simply washed with ethanol under an Ar atmosphere, and the reaction was again performed with the catalyst; however, the activity of the catalysis was significantly low (The yield of **2a** was 12%) (Table S6, entry 2). The Ni K-edge XANES analysis of the retrieved catalyst revealed that the Ni species in used Ni–Pd/HAP was partially oxidized (Fig. S8, ESI†).^{S3} As for the Pd species, the Pd K-edge XANES spectrum of used Ni–Pd/HAP resembles the previously reported spectrum of PdS (Fig. S9, ESI†).^{S4} Furthermore, S species of 0.66wt% (Pd/S molar ratio = ~1/1) were observed in the used Ni–Pd/HAP by elemental analysis, which is consistent with the plausible presence of PdS. Also, XRD patterns of fresh Ni–Pd/HAP and used Ni–Pd/HAP were measured to reveal the absence of Ni and/or Pd-derived bulk species and no change of the HAP support after the reaction (Fig. S10, ESI†). Thus, it is likely that the nanoparticle distribution is not changed much after the reaction. From the above, oxidation of Ni(0) species at the surface and conversion of Pd(0) species into PdS species are possible reasons for the deactivation of Ni–Pd/HAP catalysis. In fact, when this deactivated catalyst was calcined at 300 °C and then treated with NaBH₄ under an Ar atmosphere, the yield of **2a** was recovered till 72% for the reaction of **1a** (Table S6, entry 3), which supports the aforementioned reasons for the deactivation. However, the 2nd reuse of Ni–Pd/HAP via the aforementioned regeneration steps gave 49% yield of **2a** (Table S6, entry 4), which indicated the regeneration method is not sufficient.

Optimization of Catalysts and Reaction Conditions

A comparison of the ratio of Ni and Pd with fixed Ni content showed that **2a** was produced in high yields when the Ni/Pd ratio was higher than 1 (Table S7). Among examined various supported Ni–Pd catalysts, such as Ni–Pd/HAP, Ni–Pd/Al₂O₃, Ni–Pd/CeO₂, Ni–Pd/TiO₂, and Ni–Pd/ZrO₂, Ni–Pd/HAP showed the best catalytic performance, possibly because HAP's weak acid-base properties did not cause the side reactions producing disulfides (Table S8).^{S5} The effect of solvents was found to be remarkable: mesitylene was the most suitable solvent, and the other solvents, such as diglyme, DMA, NMP, DMSO, and decane, were not effective (Table S9). As for the temperature, the desired reaction proceeded well above 150 °C, whereas the yield of **2a** was greatly decreased below 140 °C

(Table S10).

Supplementary Figures



Ni foil	NiO	R_f
0.543	0.457	0.00345

Fig. S1 Linear curve fitting (LCF) of Ni-Pd/HAP.

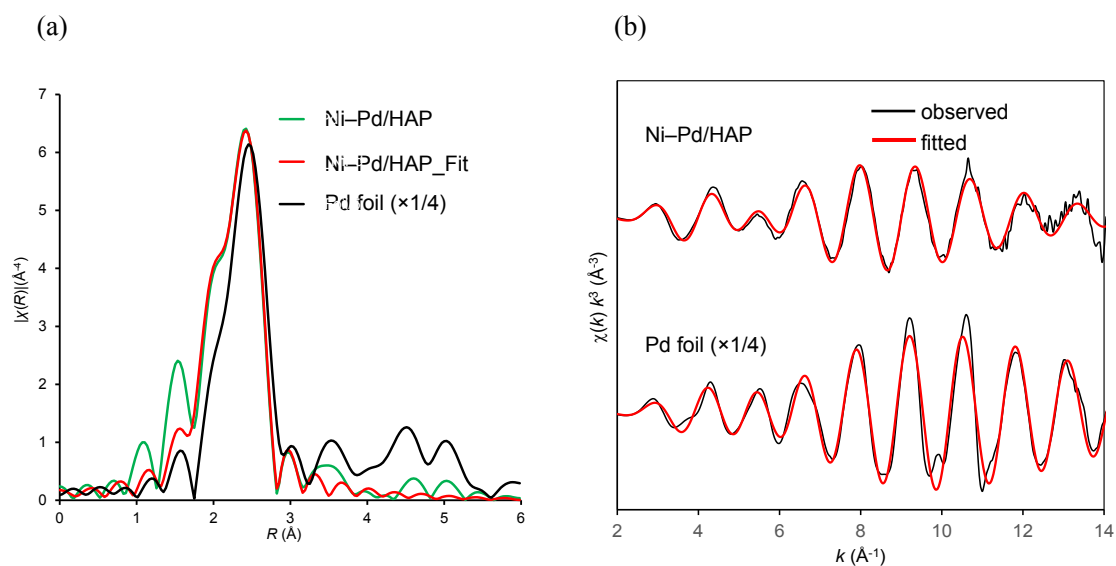


Fig. S2 (a) k^3 -weighted Fourier-transformed Pd K-edge EXAFS spectra of Ni-Pd/HAP, fitting curve, and a reference (Pd foil). FFT parameters, k -range: 3–12, window: Hanning k^3 -weighted. All R -space spectra are shown without phase correction. (b) Raw k -space Pd K-edge EXAFS spectra of Pd foil and Ni-Pd/HAP. Experimental data and fitted data are shown in black and red, respectively. FFT parameters, k -range: 3–12, window: Hanning k^3 -weighted. All k -space spectra are shown without phase correction.

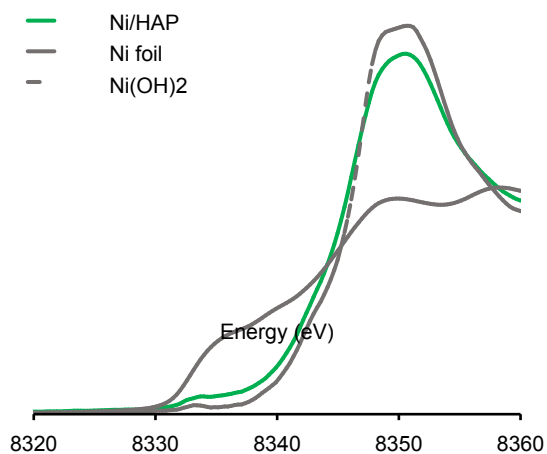


Fig. S3 Ni K-edge XANES spectra of Ni/HAP, Ni foil, and Ni(OH)₂.

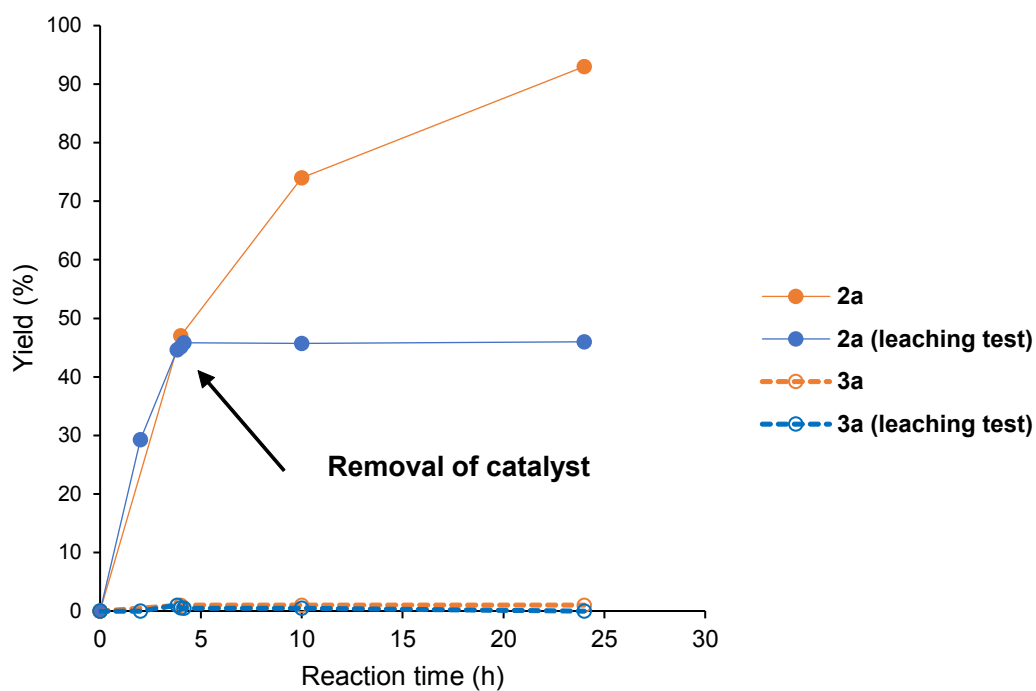


Fig. S4 Leaching test.

Reaction conditions: *p*-toluene thiol (0.5 mmol), Ni–Pd/HAP (100 mg, Ni: 4 mol%, Pd: 4 mol%), mesitylene (2 mL), H₂ (1 atm), 150 °C. Yields were determined by GC analysis using biphenyl as an internal standard.

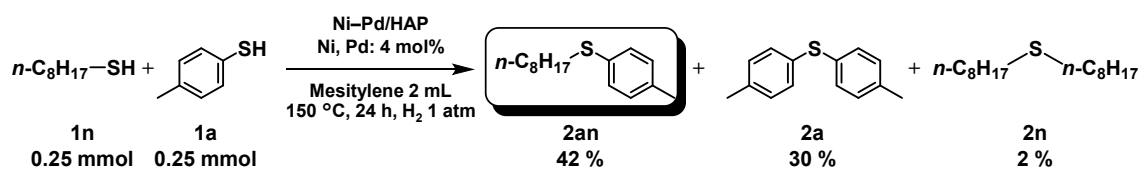


Fig. S5 Cross-metathesis of an aliphatic thiol and an aromatic thiol.

Reaction conditions are shown in this figure. Yields were determined by GC analysis using biphenyl as an internal standard.

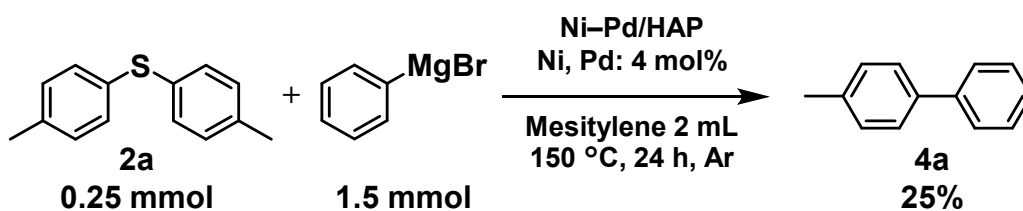


Fig. S6 Cross-coupling reaction between 2a and 4a under the conditions of the present formal C–S bond metathesis. Reaction conditions are shown in this figure. Yield of 4a was determined by GC analysis using hexadecane as an internal standard.

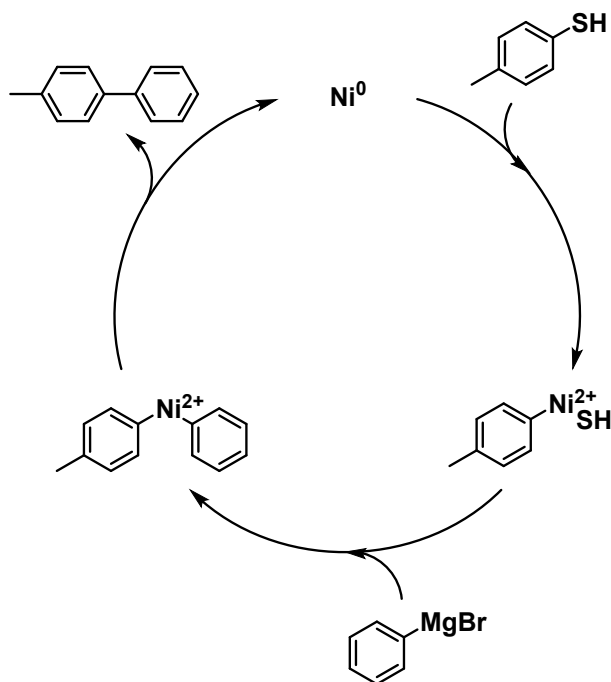


Fig. S7 Plausible mechanism of cross-coupling between thiols and Grignard reagents using Ni-Pd/HAP.

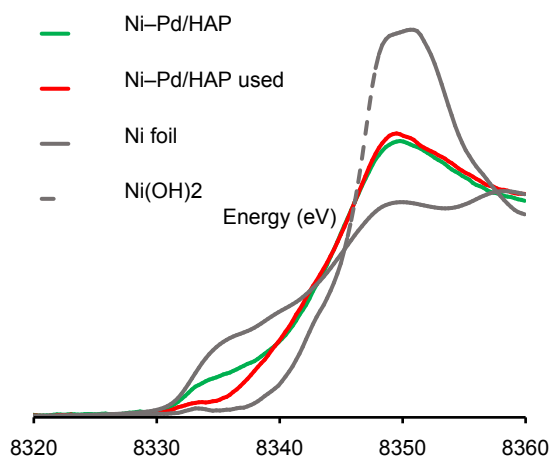


Fig. S8 Ni K-edge XANES spectra of fresh Ni-Pd/HAP, used Ni-Pd/HAP, Ni foil, and Ni(OH)₂.

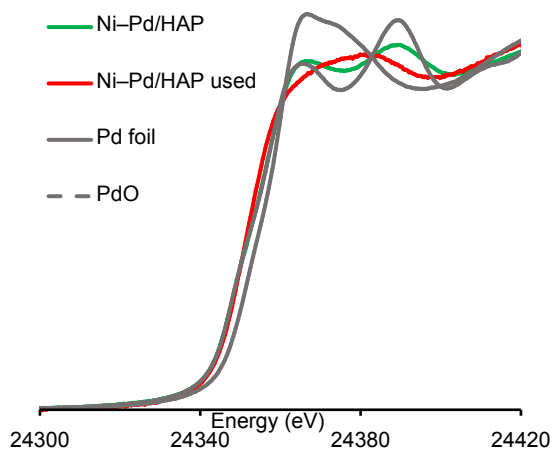


Fig. S9 Pd K-edge XANES spectra of fresh Ni-Pd/HAP, used Ni-Pd/HAP, Pd foil, and PdO.

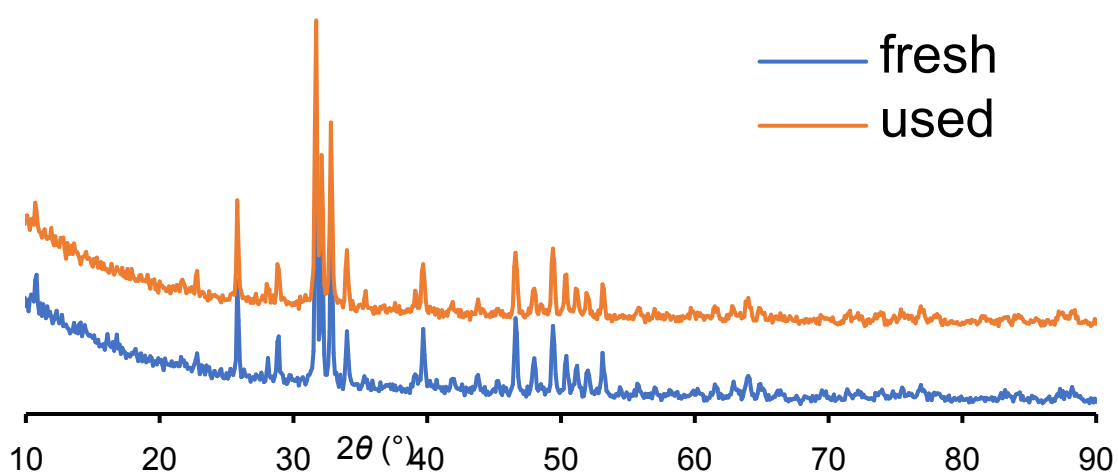


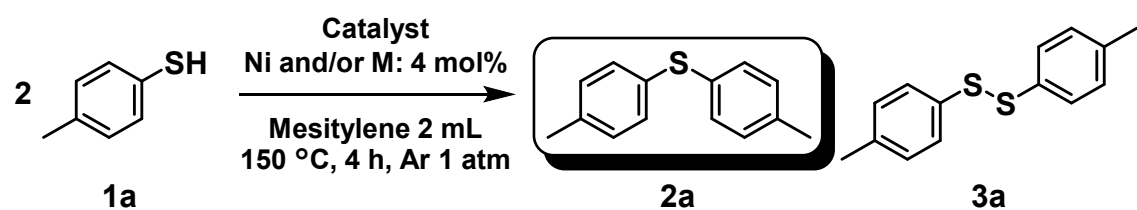
Fig. S10 XRD patterns of fresh Ni-Pd/HAP and used Ni-Pd/HAP. These spectra were obtained under an air.

Supplementary Tables

Table S1. Fitted parameters from Pd K-edge EXAFS (k^3 weighted, k range: 3–12, window: Hanning)

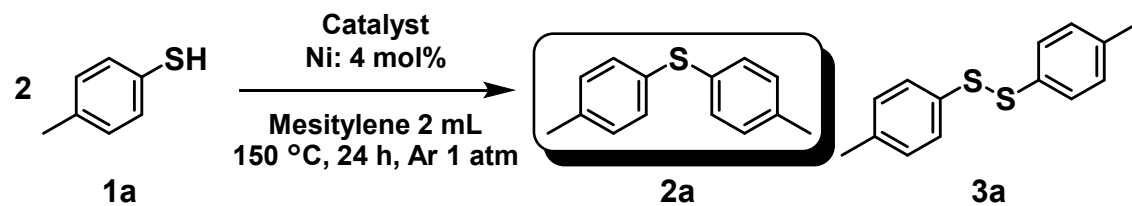
Sample	Shell	C.N.	R (Å)	ΔE_{j0} (eV)	σ (Å ²)	R_f (-)
Pd-foil	Pd–Pd	10.2	2.74	–5.68	0.00564	0.00180
Ni–Pd/HAP	Pd–Pd (Pd-foil)	5.3	2.70	–7.13	0.0109	0.0217
	Ni–Pd	1.6	2.60	–4.71	0.0109	

Table S2. Effect of catalysts on the formal C–S bond metathesis of **1a** to **2a** after 4 h of the reactions



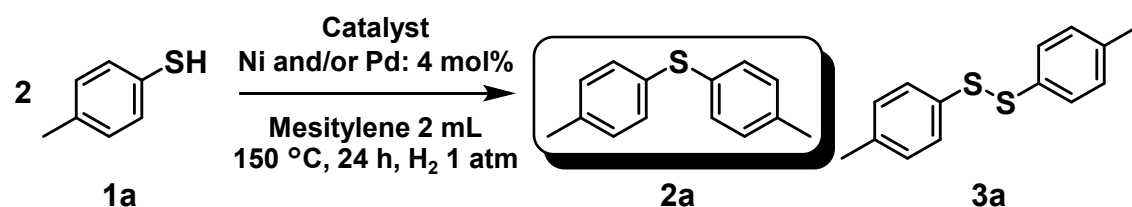
Entry	Catalyst	Yield (%)	
		2a	3a
1	Ni/HAP	35	5
2	Ni–Pd/HAP	44	<1
3 ^a	Ni–Pd/HAP	47	2
4	Ni–Ru/HAP	31	3
5 ^a	Ni–Ru/HAP	31	3
6 ^b	Ni/HAP	57	20
7 ^b	Ni–Pd/HAP	75	4
8 ^{a,b}	Ni–Pd/HAP	97	1
9 ^b	Ni–Ru/HAP	45	18
10 ^{a,b}	Ni–Ru/HAP	67	2

Reaction conditions: **1a** (0.5 mmol), catalyst (Ni and/or metal: 4 mol%), mesitylene (2 mL), Ar (1 atm), 150 °C, 4 h. Yields were determined by GC analysis using biphenyl as an internal standard. ^aH₂ (1 atm). ^b24 h.

Table S3. The effect of bimetallic catalysts on the formal C–S bond metathesis of **1a** to **2a**

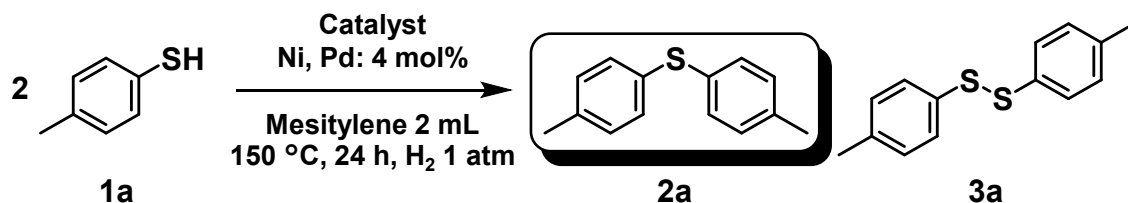
Entry	Catalyst	Yield (%)	
		2a	3a
1	Ni/HAP	57	20
2	Ni–Cu/HAP	4	3
3	Ni–Rh/HAP	42	20
4	Ni–Ru/HAP	38	17
5	Ni–Pt/HAP	8	21
6	Ni–Pd/HAP	75	4

Reaction conditions: **1a** (0.5 mmol), catalyst (Ni and/or M: 4 mol%), mesitylene (2 mL), Ar (1 atm), 150 °C, 24 h. Yields were determined by GC analysis using biphenyl as an internal standard.

Table S4. Effect of catalysts on the formal C–S bond metathesis of **1a** to **2a** under an H₂ atmosphere

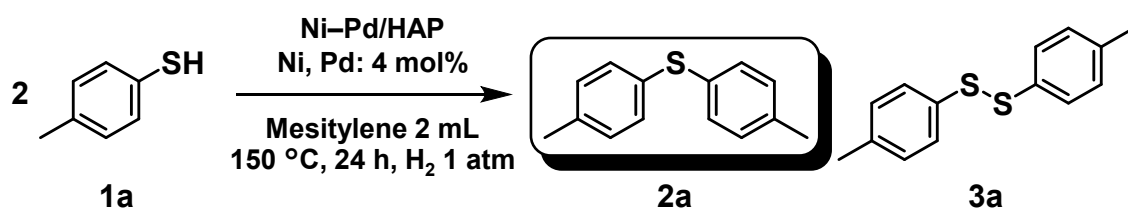
Entry	Catalyst	Yield (%)	
		2a	3a
1	Ni/HAP	60	9
2	Pd/HAP	6	1
3	Ni/HAP+Pd/HAP	99	<1

Reaction conditions: **1a** (0.5 mmol), catalyst (Ni and/or Pd: 4 mol%), mesitylene (2 mL), H₂ (1 atm), 150 °C, 24 h. Yields were determined by GC analysis using biphenyl as an internal standard.

Table S5. Amount of leaching metal species under the reaction conditions

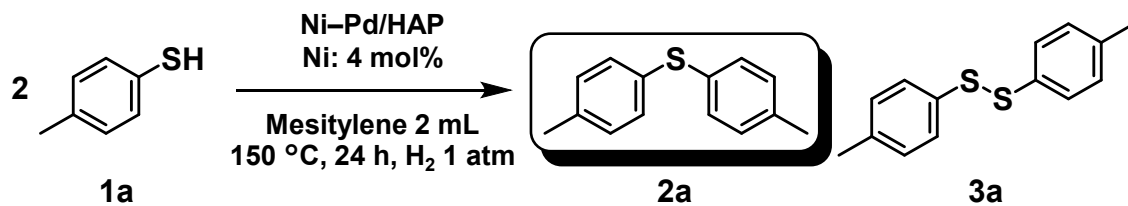
Entry	Catalyst	Time	Leaching amount (%)	
			Ni	Pd
1	Ni-Pd/HAP	1 min	2.2	n.d.
2	Ni-Pd/HAP	24 h	n.d.	n.d.
3	Ni/HAP+Pd/HAP	1 min	16	n.d.
4	Ni/HAP+Pd/HAP	24 h	n.d.	n.d.

Reaction conditions: **1a** (0.5 mmol), catalyst (Ni: 4 mol%, Pd: 4 mol%), mesitylene (2 mL), H₂ (1 atm), 150 °C, 24 h.

Table S6. Reuse test

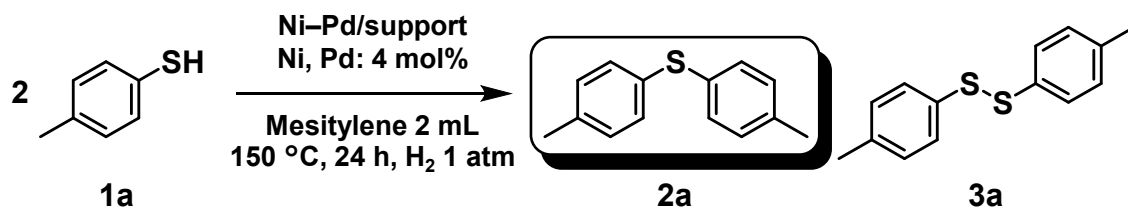
Entry	Catalyst	Yield (%)	
		2a	3a
1	fresh	97	<1
2	used	12	4
3	used ^[a]	72	1
4	used ^[a,b]	49	1

Reaction conditions: **1a** (0.5 mmol), Ni-Pd/HAP (100 mg, Ni: 4 mol%, Pd: 4 mol%), mesitylene (2 mL), H₂ (1 atm), 150 °C, 24 h. [a] Calcinated at 300 °C for 2 h under an air atmosphere and reduced with NaBH₄ (120 mg) under an Ar atmosphere. [b] 2nd reuse. Yields were determined by GC analysis using biphenyl as an internal standard.

Table S7. Effect of Ni/Pd ratio on the formal C–S bond metathesis of **1a** to **2a**

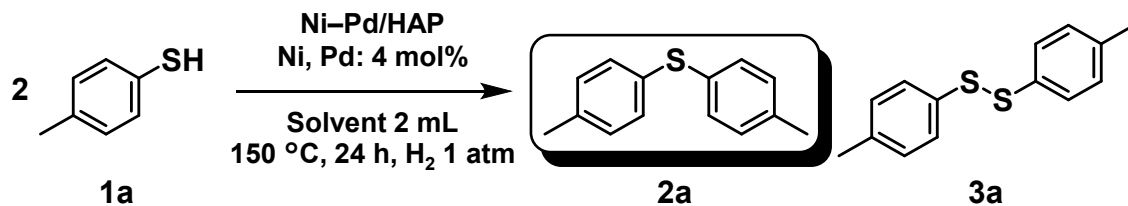
Entry	Pd (mol%)	Yield (%)	
		2a	3a
1	2	85	1
2	4	97	1
3	8	99	<1

Reaction conditions: **1a** (0.5 mmol), Ni-Pd/HAP (100 mg, Ni: 4 mol%), mesitylene (2 mL), H₂ (1 atm), 150 °C, 24 h. Yields were determined by GC analysis using biphenyl as an internal standard.

Table S8. Effect of supports on the formal C–S bond metathesis of **1a** to **2a**

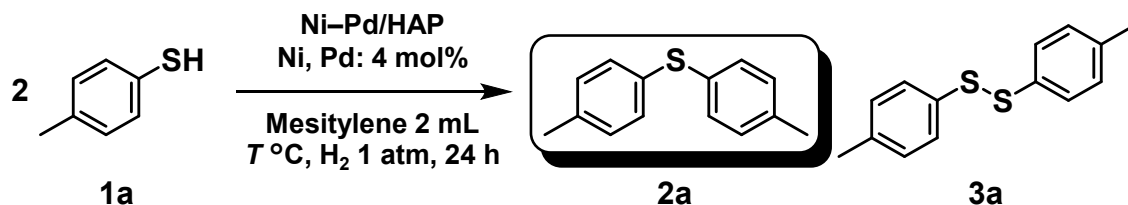
Entry	Support	Yield (%)	
		2a	3a
1	HAP	97	1
2	Al ₂ O ₃	54	7
3	CeO ₂	34	23
4	TiO ₂	54	9
5	ZrO ₂	42	3

Reaction conditions: **1a** (0.5 mmol), Ni-Pd/support (100 mg, Ni: 4 mol%, Pd: 4 mol%), mesitylene (2 mL), H₂ (1 atm), 150 °C, 24 h. Yields were determined by GC analysis using biphenyl as an internal standard.

Table S9. Effect of solvents on the formal C–S bond metathesis of **1a** to **2a**

Entry	Solvent	Yield (%)	
		2a	3a
1	Mesitylene	97	1
2	Diglyme	56	9
3	Decane	18	8
4	DMA	28	9
5	DMSO	7	24
6	NMP	19	26

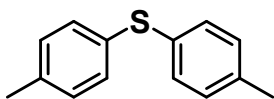
Reaction conditions: **1a** (0.5 mmol), Ni–Pd/HAP (100 mg, Ni: 4 mol%, Pd: 4 mol%), solvent (2 mL), H₂ (1 atm), 150 °C, 24 h. Yields were determined by GC analysis using biphenyl as an internal standard.

Table S10. Effect of reaction temperatures on the formal C–S bond metathesis of **1a** to **2a**

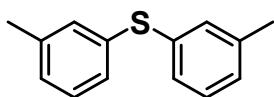
Entry	Temperature (°C)	Yield (%)	
		2a	3a
1	140	35	13
2	150	97	1
3	160	>99	1

Reaction conditions: **1a** (0.5 mmol), Ni–Pd/HAP (100 mg, Ni: 4 mol%, Pd: 4 mol%), mesitylene (2 mL), H₂ (1 atm), 24 h. Yields were determined by GC analysis using biphenyl as an internal standard.

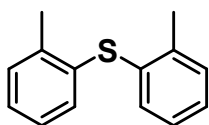
Spectral Data



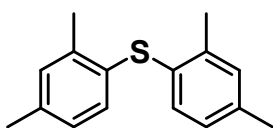
Di-*p*-tolyl sulfide (2a) (CAS No. 620-94-0): 97% GC yield, 75% isolated yield (Table 2). GC conditions and analysis: InertCap5 capillary column, 0.25 mm×60 m, GL Science Inc.; carrier gas (N₂) flow rate, 2.4 mL·min⁻¹, initial column temp., 100 °C; final column temp., 280 °C, progress rate, 10 °C·min⁻¹, injection temp., 280 °C; detection temp., 280 °C; retention time, 18.5 min; relative sensitivity for quantification (vs biphenyl, internal standard), 1.13 (determined by calibration curve). Isolated as white powder (Silica gel column chromatography; eluent: hexane, *R_f* = 0.50). ¹H NMR (500 MHz, CDCl₃, TMS): δ 7.23–7.21 (m, 4H, Ar), 7.09–7.07 (m, 4H, Ar), 2.31 (s, 6H, CH₃). ¹³C{¹H}NMR (125 MHz, CDCl₃, TMS): δ 137.0, 132.8, 131.2, 130.0, 21.2. These NMR spectral data accord with that in previously reported.^{S6} MS (70 eV, EI): *m/z* (%): 216 (6), 215 (17), 214 (100) [*M*⁺], 213 (15), 200 (6), 199 (38), 198 (16), 197 (8), 184 (22), 181 (13), 166 (6), 165 (9), 106 (6), 105 (16), 91 (27), 89 (5), 77 (7), 65 (14), 63 (5).



Di-*m*-tolyl sulfide (2b) (CAS No. 3111-77-1): 80% GC yield, 51% isolated yield (Table 2). GC conditions and analysis: InertCap5 capillary column, 0.25 mm×60 m, GL Science Inc.; carrier gas (N₂) flow rate, 2.4 mL·min⁻¹, initial column temp., 100 °C; final column temp., 280 °C, progress rate, 10 °C·min⁻¹, injection temp., 280 °C; detection temp., 280 °C; retention time, 18.6 min; relative sensitivity for quantification (vs biphenyl, internal standard), 1.13 (estimated to be equal to that of **2a**). Isolated as colorless liquid (Silica gel column chromatography; eluent: hexane, *R_f* = 0.50). ¹H NMR (500 MHz, CDCl₃, TMS): δ 7.23–7.16 (m, 4H, Ar), 7.13–7.11 (m, 2H, Ar), 7.05–7.03 (m, 2H, Ar), 2.30 (s, 6H, CH₃). ¹³C{¹H}NMR (125 MHz, CDCl₃, TMS): δ 135.7, 131.7, 131.2, 129.1, 128.2, 128.0, 21.4. These NMR spectral data accord with that in previously reported.^{S6} MS (70 eV, EI): *m/z* (%): 216 (6), 215 (16), 214 (100) [*M*⁺], 213 (11), 200 (5), 199 (30), 198 (17), 197 (9), 185 (5), 184 (28), 166 (7), 165 (9), 121 (5), 106 (5), 105 (15), 91 (11), 89 (6), 77 (7), 65 (17), 63 (7), 51 (5).

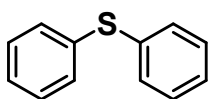


Di-*o*-tolyl sulfide (2c) (CAS No. 4537-05-7): 53% GC yield, 37% isolated yield (Table 2). GC conditions and analysis: InertCap5 capillary column, 0.25 mm×60 m, GL Science Inc.; carrier gas (N₂) flow rate, 2.4 mL·min⁻¹, initial column temp., 100 °C; final column temp., 280 °C, progress rate, 10 °C·min⁻¹, injection temp., 280 °C; detection temp., 280 °C; retention time, 17.7 min; relative sensitivity for quantification (vs biphenyl, internal standard), 1.13 (estimated to be equal to that of **2a**). Isolated as colorless liquid (Silica gel column chromatography; eluent: hexane, *R_f* = 0.50). ¹H NMR (500 MHz, CDCl₃, TMS): δ 7.24–7.22 (m, 2H, Ar), 7.18–7.15 (m, 2H, Ar), 7.09–7.04 (m, 4H, Ar), 2.38 (s, 6H, CH₃). ¹³C{¹H}NMR (125 MHz, CDCl₃, TMS): δ 139.0, 134.4, 131.2, 130.6, 127.2, 126.8, 20.5. These NMR spectral data accord with that in previously reported.^{S6} MS (70 eV, EI): *m/z* (%): 216 (6), 215 (17), 214 (100) [*M*⁺], 199 (19), 198 (6), 197 (10), 184 (12), 166 (7), 165 (10), 123 (11), 122 (58), 121 (36), 106 (6), 105 (19), 92 (5), 91 (27), 89 (9), 78 (10), 77 (9), 65 (18), 63 (6), 51 (5).



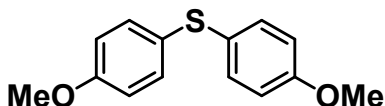
Bis-(2,4-dimethylphenyl) sulfide (2d) (CAS No. 20058-03-1): 53% GC yield, 38% isolated yield (Table 2). GC conditions and analysis: InertCap5 capillary column, 0.25 mm×60 m, GL Science Inc.; carrier gas (N₂) flow rate, 2.4 mL·min⁻¹, initial column temp., 100 °C; final column temp., 280

°C, progress rate, 10 °C·min⁻¹, injection temp., 280 °C; detection temp., 280 °C; retention time, 20.0 min; relative sensitivity for quantification (vs biphenyl, internal standard), 1.30 (estimated by **2a** and the effective carbon number concept^{S7}). Isolated as colorless liquid (Silica gel column chromatography; eluent: hexane, $R_f = 0.40$). ¹H NMR (500 MHz, CDCl₃, TMS): δ 7.04 (s, 2H, Ar), 6.94 (d, $J = 8.0$ Hz, 2H, Ar), 6.90 (d, $J = 8.0$ Hz, 2H, Ar), 2.33 (s, 6H, CH₃), 2.29 (s, 6H, CH₃). ¹³C{¹H}NMR (125 MHz, CDCl₃, TMS): δ 138.8, 136.9, 131.4, 131.3, 131.2, 127.5, 21.0, 20.4. MS (70 eV, EI): m/z (%): 244 (6), 243 (18), 242 (100) [M^+], 227 (12), 225 (6), 212 (12), 211 (6), 179 (5), 178 (5), 137 (10), 136 (62), 135 (33), 121 (7), 119 (7), 106 (5), 105 (26), 103 (9), 92 (9), 91 (19), 79 (10), 78 (7), 77 (22), 65 (6), 51 (5).



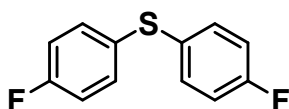
Diphenyl sulfide (2e) (CAS No. 139-66-2): 68% GC yield, 53% isolated yield (Table 2). GC conditions and analysis: InertCap5 capillary column, 0.25 mm×60 m, GL Science Inc.; carrier gas (N₂) flow rate, 2.4 mL·min⁻¹, initial column temp., 100 °C; final column temp., 280 °C, progress rate, 10 °C·min⁻¹, injection

temp., 280 °C; detection temp., 280 °C; retention time, 15.8 min; relative sensitivity for quantification (vs biphenyl, internal standard), 0.963 (estimated by **2a** and the effective carbon number concept^{S7}). Isolated as colorless liquid (Silica gel column chromatography; eluent: hexane, $R_f = 0.50$). ¹H NMR (500 MHz, CDCl₃, TMS): δ 7.35–7.33 (m, 4H, Ar), 7.31–7.28 (m, 4H, Ar), 7.25–7.22 (m, 2H, Ar). ¹³C{¹H}NMR (125 MHz, CDCl₃, TMS): δ 135.9, 131.1, 129.3, 127.1. MS (70 eV, EI): m/z (%): 188 (5), 187 (17), 186 (100) [M^+], 185 (77), 184 (33), 171 (5), 152 (9), 109 (5), 92 (11), 77 (13), 69 (6), 65 (10), 51 (22), 50 (5). These NMR and GC-MS spectral data accord with those in previously reported.^{S6,S8}



4,4'-Dimethoxy diphenyl sulfide (2f) (CAS No. 3393-77-9): 62% GC yield, 61% isolated yield (Table 2). GC conditions and analysis: InertCap5 capillary column, 0.25 mm×60 m, GL

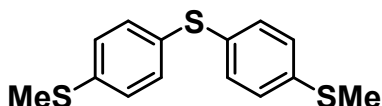
Science Inc.; carrier gas (N₂) flow rate, 2.4 mL·min⁻¹, initial column temp., 100 °C; final column temp., 280 °C, progress rate, 10 °C·min⁻¹, injection temp., 280 °C; detection temp., 280 °C; retention time, 22.2 min; relative sensitivity for quantification (vs biphenyl, internal standard), 0.911 (determined by calibration curve). Isolated as colorless liquid (Silica gel column chromatography; eluent: hexane/ethyl acetate = 93/7, $R_f = 0.50$). ¹H NMR (500 MHz, CDCl₃, TMS): δ 7.28–7.26 (m, 4H, Ar), 6.83–6.81 (m, 4H, Ar), 3.77 (s, 6H, CH₃). ¹³C{¹H}NMR (125 MHz, CDCl₃, TMS): δ 159.1, 132.8, 127.5, 114.9, 55.4. These NMR spectral data accord with that in previously reported.^{S6} MS (70 eV, EI): m/z (%): 248 (6), 247 (16), 246 (100) [M^+], 232 (6), 231 (41), 215 (6), 214 (10), 203 (8), 200 (5), 199 (7), 188 (6), 172 (6), 171 (9), 160 (7), 159 (5), 139 (7), 123 (5), 115 (7), 96 (5), 95 (5), 92 (5), 77 (5), 64.05 (7), 63 (7).



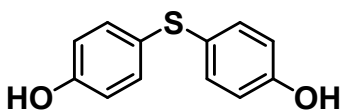
4,4'-Difluoro diphenyl sulfide (2g) (CAS No. 404-38-6): 78% GC yield, 69% isolated yield (Table 2). GC conditions and analysis: InertCap5 capillary column, 0.25 mm×60 m, GL Science Inc.; carrier gas (N₂) flow rate, 2.4 mL·min⁻¹, initial column temp., 100 °C; final column temp., 280

°C, progress rate, 10 °C·min⁻¹, injection temp., 280 °C; detection temp., 280 °C; retention time, 15.2 min; relative sensitivity for quantification (vs biphenyl, internal standard), 0.921 (estimated by **2a** and the effective carbon number concept^{S7}). Isolated as colorless liquid (Silica gel column chromatography; eluent: hexane, $R_f = 0.50$). ¹H NMR (500 MHz, CDCl₃, TMS): δ 7.31–7.28 (m, 4H,

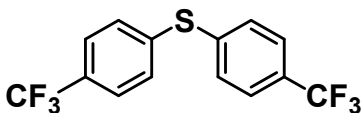
Ar), 7.02–6.98 (m, 4H, Ar). $^{13}\text{C}\{^1\text{H}\}$ NMR (125 MHz, CDCl_3 , TMS): δ 162.3 (d, $J = 247.1$ Hz), 133.1 (d, $J = 8.4$ Hz), 131.1, 116.5 (d, $J = 21.6$ Hz). These NMR spectral data accord with that in previously reported.^{S9} MS (70 eV, EI): m/z (%): 223 (9), 222 (53) [M^+], 221 (27), 220 (11), 203 (7), 202 (11), 201 (9), 190 (6), 189 (7), 127 (21), 126 (9), 120 (5), 111 (5), 102 (5), 101 (10), 96 (5), 95 (26), 94 (9), 93 (8), 87 (5), 84 (9), 83 (100), 82 (10), 81 (12), 76 (8), 75 (89), 74 (22), 70 (6), 69 (50), 68 (12), 63 (23), 62 (12), 58 (6), 57 (50), 51 (19), 50 (41).



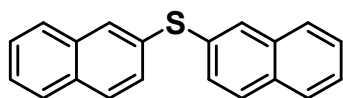
4,4'-Di-(methylthio)-diphenyl sulfide (2h) (CAS No. 125877-23-8): 95% GC yield, 71% isolated yield (Table 2). GC conditions and analysis: InertCap5 capillary column, 0.25 mm \times 60 m, GL Science Inc.; carrier gas (N_2) flow rate, 2.4 mL \cdot min $^{-1}$, initial column temp., 100 $^\circ\text{C}$; final column temp., 280 $^\circ\text{C}$, progress rate, 10 $^\circ\text{C}\cdot$ min $^{-1}$, injection temp., 280 $^\circ\text{C}$; detection temp., 280 $^\circ\text{C}$; retention time, 29.6 min; relative sensitivity for quantification (vs biphenyl, internal standard), 0.911 (estimated to be equal to that of **2f**). Isolated as colorless liquid (Silica gel column chromatography; eluent: hexane/ethyl acetate = 93/7, $R_f = 0.50$). ^1H NMR (500 MHz, CDCl_3 , TMS): δ 7.25–7.22 (m, 4H, Ar), 7.19–7.15 (m, 4H, Ar), 2.46 (s, 6H, CH_3). $^{13}\text{C}\{^1\text{H}\}$ NMR (125 MHz, CDCl_3 , TMS): δ 137.9, 132.3, 131.6, 127.3, 15.9. MS (70 eV, EI): m/z (%): 281 (6), 280 (15), 279 (18), 278 (100) [M^+], 263 (20), 233 (5), 232 (9), 231 (49), 216 (18), 215 (7), 207 (6), 184 (15), 171 (7), 155 (6), 140 (7), 139 (12), 108 (9), 96 (5), 73 (6), 69 (5).



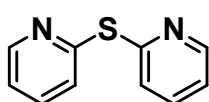
4,4'-Dihydroxy diphenyl sulfide (2i) (CAS No. 2664-63-3): 64% GC yield (Table 2). GC conditions and analysis: InertCap5 capillary column, 0.25 mm \times 60 m, GL Science Inc.; carrier gas (N_2) flow rate, 2.4 mL \cdot min $^{-1}$, initial column temp., 100 $^\circ\text{C}$; final column temp., 280 $^\circ\text{C}$, progress rate, 10 $^\circ\text{C}\cdot$ min $^{-1}$, injection temp., 280 $^\circ\text{C}$; detection temp., 280 $^\circ\text{C}$; retention time, 23.7 min; relative sensitivity for quantification (vs biphenyl, internal standard), 0.855 (estimated by **2a** and the effective carbon number concept^{S7}). MS (70 eV, EI): m/z (%): 220 (6), 219 (16), 218 (100) [M^+], 217 (23), 201 (7), 198 (7), 189 (9), 187 (5), 186 (17), 185 (14), 171 (7), 157 (28), 131 (10), 129 (8), 128 (13), 127 (17), 126 (8), 125 (31), 124 (5), 118 (7), 115 (13), 109 (6), 102 (7), 100 (13), 98 (8), 97 (44), 96 (7), 95 (13), 94 (5), 92 (6), 91 (6), 86 (13), 85 (16), 82 (10), 81 (51), 78 (5), 77 (10), 75 (8), 74 (14), 73 (6), 71 (19), 70 (32), 69 (44), 68 (8), 66 (16), 65 (83), 64 (35), 63 (81), 62 (37), 61 (11), 58 (6), 55 (22), 54 (6), 53 (84), 52 (8), 51 (25), 50 (25). This GC-MS spectral data accords with those previously reported.^{S8}



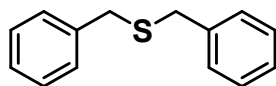
4,4'-Di-(trifluoromethyl)-diphenyl sulfide (2j) (CAS No. 90141-51-8): 23% GC yield (Table 2). GC conditions and analysis: InertCap5 capillary column, 0.25 mm \times 60 m, GL Science Inc.; carrier gas (N_2) flow rate, 2.4 mL \cdot min $^{-1}$, initial column temp., 100 $^\circ\text{C}$; final column temp., 280 $^\circ\text{C}$, progress rate, 10 $^\circ\text{C}\cdot$ min $^{-1}$, injection temp., 280 $^\circ\text{C}$; detection temp., 280 $^\circ\text{C}$; retention time, 17.4 min; relative sensitivity for quantification (vs biphenyl, internal standard), 0.998 (estimated by **2a** and the effective carbon number concept^{S7}). MS (70 eV, EI): m/z (%): 324 (5), 323 (17), 322 (100) [M^+], 303 (19), 301 (20), 253 (14), 252 (15), 234 (8), 233 (55), 185 (5), 184 (35), 158 (5), 157 (15), 145 (12), 133 (5), 126 (6), 125 (14), 114 (11), 108 (14), 95 (20), 82 (5), 76 (5), 75 (24), 74 (7), 69 (40), 63 (9), 57 (6), 51 (7), 50 (13).



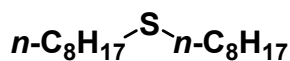
2,2'-Dinaphthyl sulfide (2k) (CAS No. 613-81-0): 65% GC yield, 56% isolated yield (Table 2). GC conditions and analysis: InertCap5 capillary column, 0.25 mm×60 m, GL Science Inc.; carrier gas (N₂) flow rate, 2.4 mL·min⁻¹, initial column temp., 100 °C; final column temp., 280 °C, progress rate, 10 °C·min⁻¹, injection temp., 280 °C; detection temp., 280 °C; retention time, 38.6 min; relative sensitivity for quantification (vs biphenyl, internal standard), 1.77 (estimated by **2a** and the effective carbon number concept^{S7}). Isolated as white solid (Silica gel column chromatography; eluent: hexane, *R_f*=0.45). ¹H NMR (500 MHz, CDCl₃, TMS): δ 7.87–7.86 (m, 2H, Ar), δ 7.81–7.71 (m, 6H, Ar), 7.47–7.44 (m, 6H, Ar). ¹³C {¹H} NMR (125 MHz, CDCl₃, TMS): δ 133.9, 133.2, 132.4, 129.9, 129.0, 128.8, 127.9, 127.5, 126.7, 126.3. These NMR spectral data accord with that in previously reported.^{S10} MS (70 eV, EI): *m/z* (%): 288 (7), 287 (23), 286 (100) [*M*⁺], 285 (47), 284 (23), 283 (5), 254 (5), 253 (15), 252 (22), 143 (11), 142 (13), 127 (9), 126 (14), 115 (20), 77 (7).



2,2'-Dipyridyl sulfide (2l) (CAS No. 4262-06-0): 17% GC yield (Table 2). GC conditions and analysis: InertCap5 capillary column, 0.25 mm×60 m, GL Science Inc.; carrier gas (N₂) flow rate, 2.4 mL·min⁻¹, initial column temp., 100 °C; final column temp., 280 °C, progress rate, 10 °C·min⁻¹, injection temp., 280 °C; detection temp., 280 °C; retention time, 17.9 min; relative sensitivity for quantification (vs biphenyl, internal standard), 0.73 (estimated by **2a** and the effective carbon number concept^{S7}). MS (70 eV, EI): *m/z* (%): 189 (9), 188 (37) [*M*⁺], 187 (100), 118 (5), 117 (5), 94 (5), 83 (6), 82 (5), 79 (10), 78 (29), 67 (7), 52 (14), 51 (44), 50 (12). This GC-MS spectral data accords with those in previously reported.^{S11,S12}



Dibenzyl sulfide (2m) (CAS No. 538-74-9): 84% GC yield (Table 2). GC conditions and analysis: InertCap5 capillary column, 0.25 mm×60 m, GL Science Inc.; carrier gas (N₂) flow rate, 2.4 mL·min⁻¹, initial column temp., 100 °C; final column temp., 280 °C, progress rate, 10 °C·min⁻¹, injection temp., 280 °C; detection temp., 280 °C; retention time, 17.8 min; relative sensitivity for quantification (vs biphenyl, internal standard), 1.13 (estimated to be equal to that of **2a**). MS (70 eV, EI): *m/z* (%): 214 (24) [*M*⁺], 123 (21), 122 (13), 92 (21), 91 (100), 77 (7), 65 (22), 63 (5), 51 (6). This GC-MS spectral data accords with that in previously reported.^{S8}

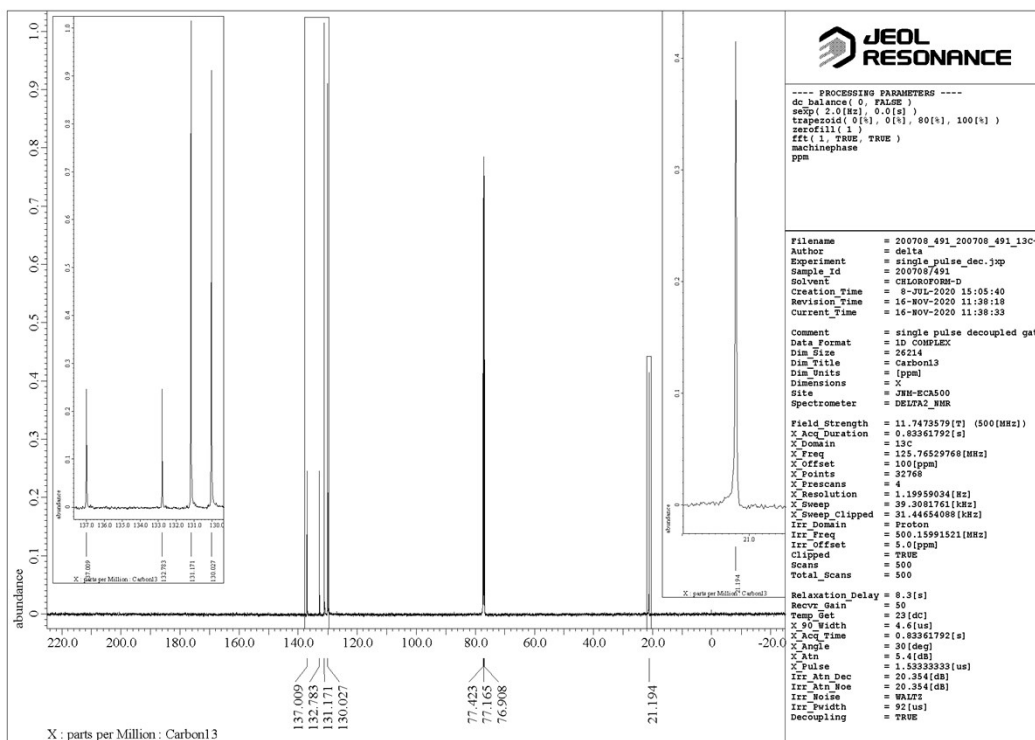
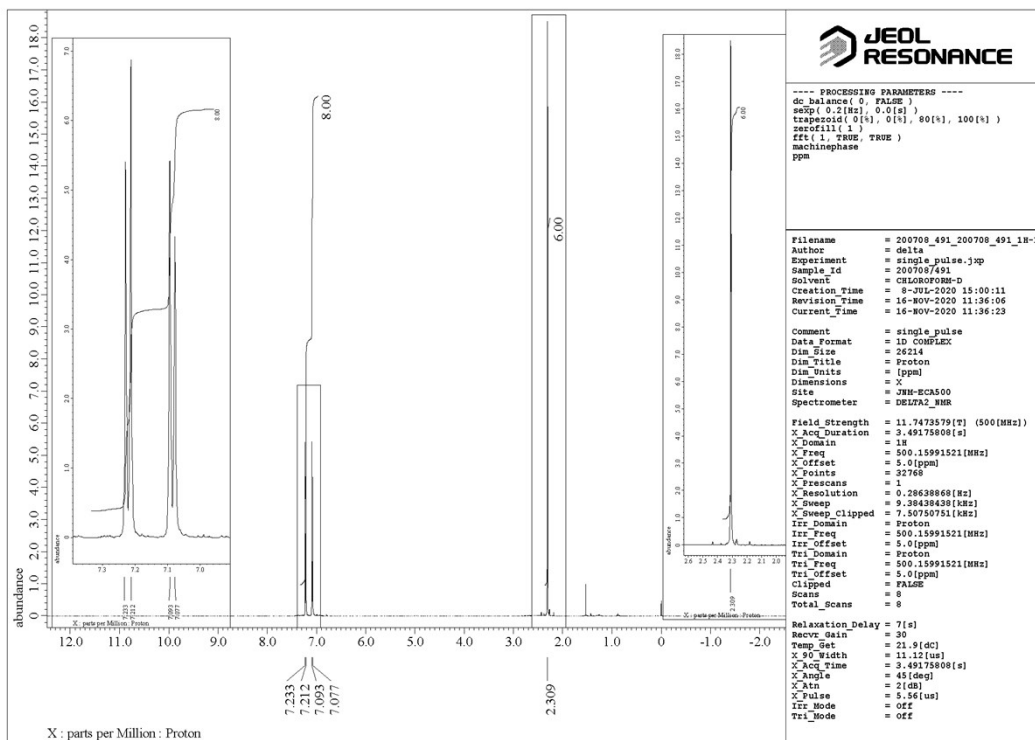
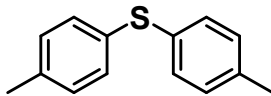


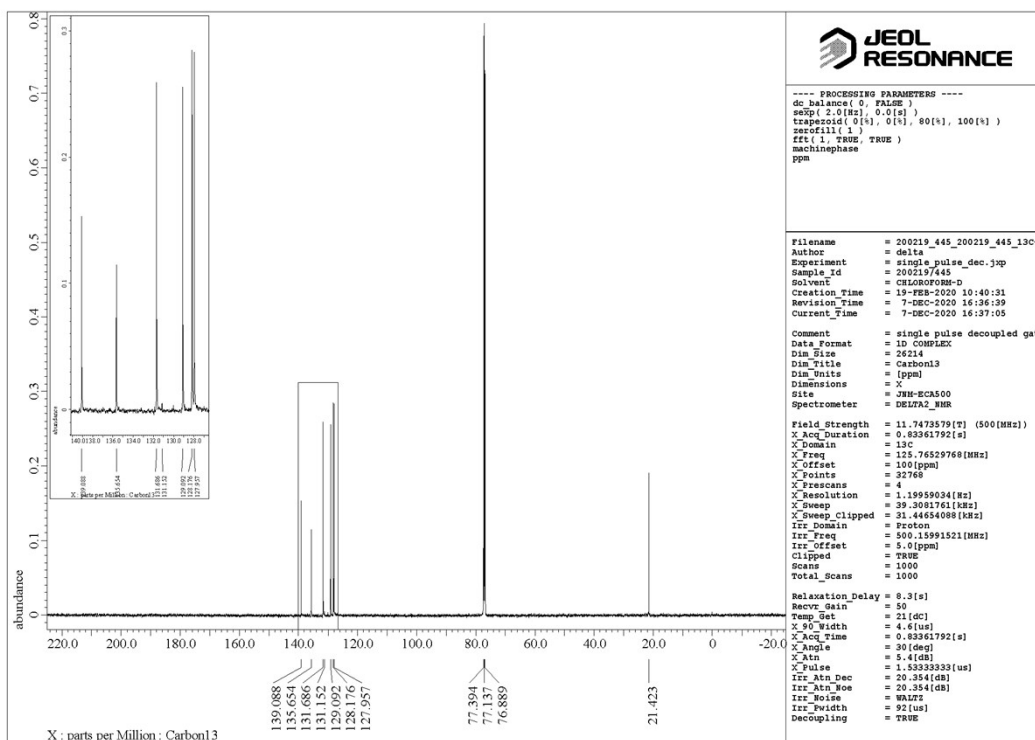
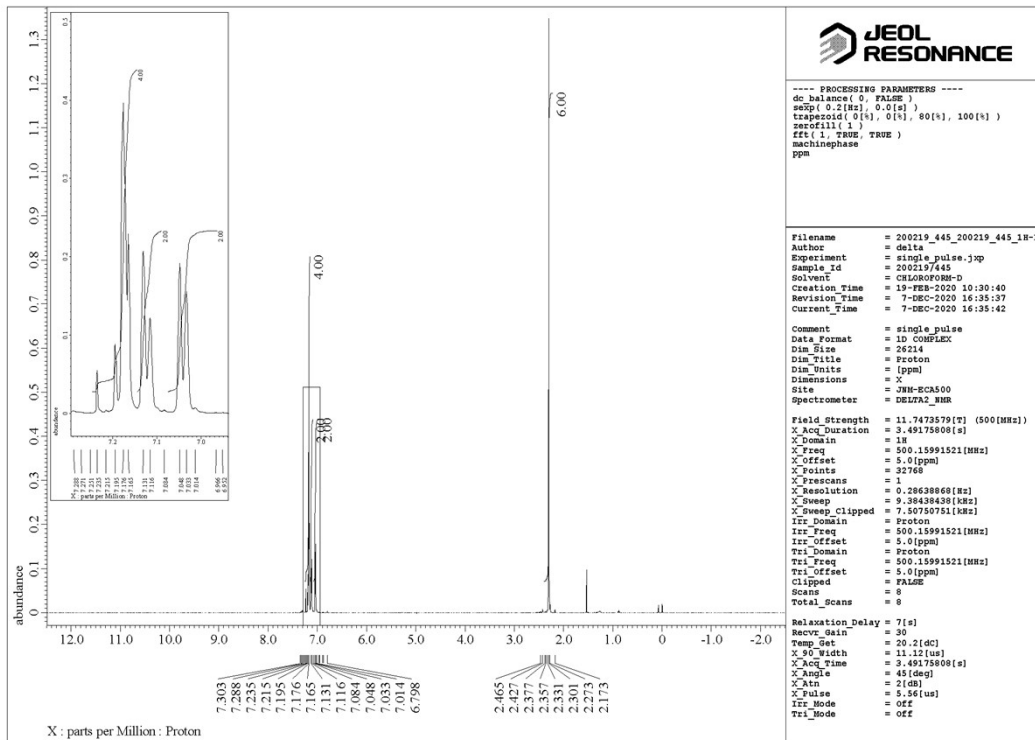
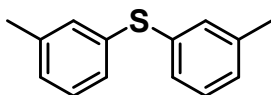
Di-*n*-Octyl sulfide (2n) (CAS No. 2690-08-6): 27% GC yield (Table 2). GC conditions and analysis: InertCap5 capillary column, 0.25 mm×60 m, GL Science Inc.; carrier gas (N₂) flow rate, 2.4 mL·min⁻¹, initial column temp., 100 °C; final column temp., 280 °C, progress rate, 10 °C·min⁻¹, injection temp., 280 °C; detection temp., 280 °C; retention time, 18.7 min; relative sensitivity for quantification (vs biphenyl, internal standard), 1.27 (estimated by the effective carbon number concept^{S7}) MS (70 eV, EI): *m/z* (%): 258 (17) [*M*⁺], 159 (5), 147 (7), 146 (13), 145 (100), 144 (6), 112 (20), 87 (6), 84 (15), 83 (21), 82 (9), 71 (13), 70 (24), 69 (57), 68 (6), 67 (5), 61 (19), 57 (24), 56 (21), 55 (36). This GC-MS spectral data accords with that in previously reported.^{S8}

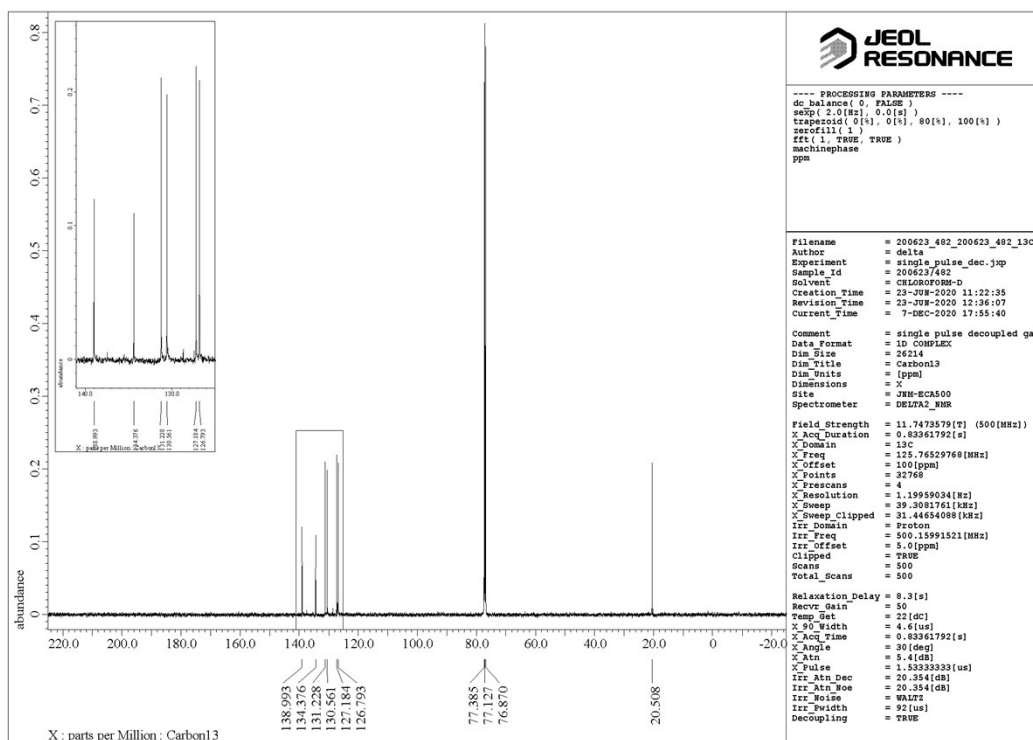
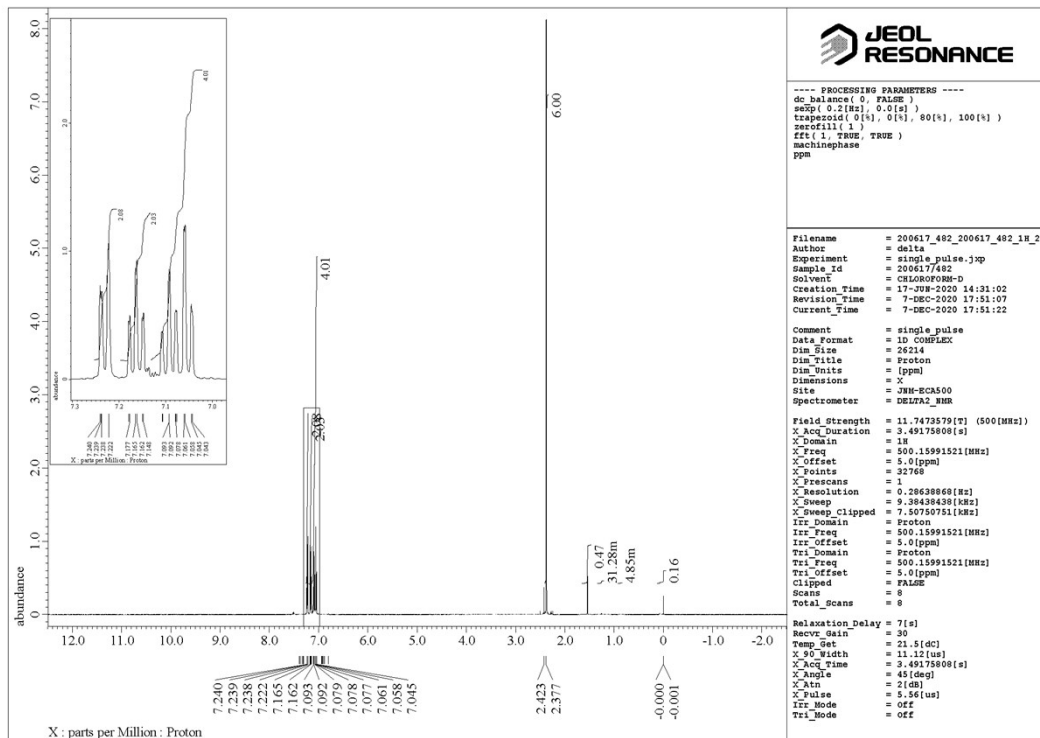
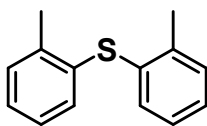
Supplementary References

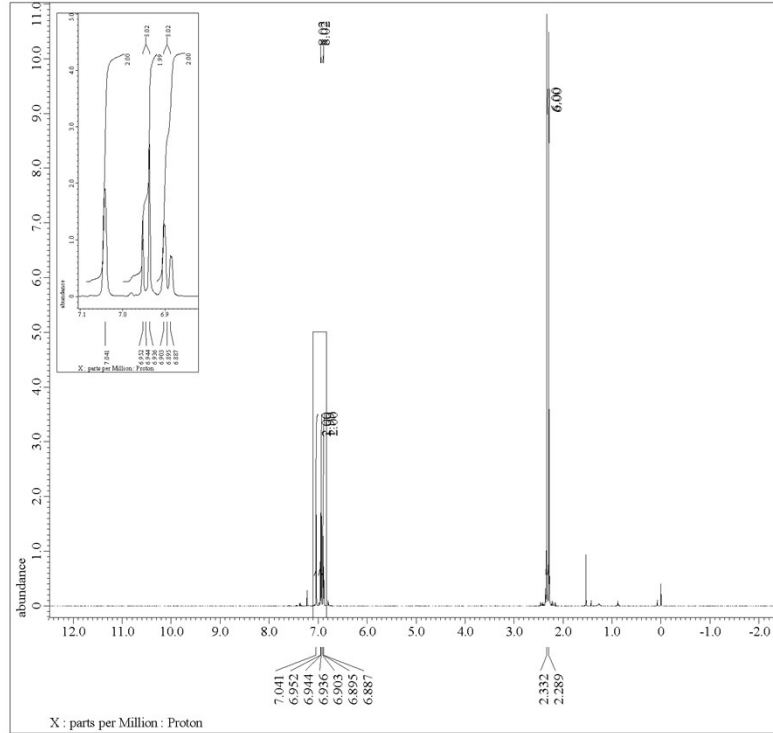
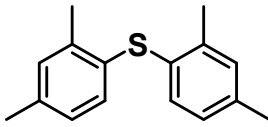
- S1 (a) J. W. Cable and Y. Tsunoda, *J. Magn. Magn. Mater.*, 1995, **140–144**, 93–94; (b) Z. Feng, V. Suresh Babu, J. Zhao and M. S. Seehra, *J. Appl. Phys.*, 1991, **70**, 6161–6163; (c) Y. Sakamoto, F. L. Chen and R.-A. McNicholl, *J. Alloys Compd.*, 1993, **192**, 145–148.
- S2 S. Karanjit, A. Jinasan, E. Samsook, R. N. Dhital, K. Motomiya, Y. Sato, K. Tohjic and H. Sakurai, *Chem. Commun.*, 2015, **51**, 12724–12727.
- S3 For examples on nickel or iron particles being partially oxidized/reduced according to pre-edge peak spectra in XANES area: (a) C. Gougoussis, M. Calandra, A. Seitsonen, Ch. Brouder, A. Shukla and F. Mauri, *Phys. Rev. B*, 2009, **79**, 045118; (b) N. V. R. A. Dharanipragada, V. V. Galvita, H. Poelman, L. C. Buelens and G. B. Marin, *AIChE J.*, 2018, **64**, 1339–1349.
- S4 Y. Li, S. Yu, D. E. Doronkin, S. Wei, M. Dan, F. Wu, L. Ye, J.-D. Grunwaldt and Y. Zhou, *J. Catal.*, 2019, **373**, 48–57.
- S5 (a) K. Kaneda and T. Mizugaki, *Energy Environ. Sci.*, 2009, **2**, 655–673. (b) Z. Boukha, J. L. Ayastuy, J. R. González-Velasco and M. A. Gutiérrez-Ortiz, *Appl. Catal. A*, 2018, **566**, 1–14. (c) C. R. Ho, S. Zheng, S. Shylesh and A. T. Bell, *J. Catal.*, 2018, **365**, 174–183. (d) Y. Matsuura, A. Ondaa, S. Ogo and K. Yanagisawa, *Catal. Today*, 2014, **226**, 192–197. (e) Y. Wan, C. Zheng, X. Lei, M. Zhuang, J. Lin, W. Hu, J. Lin, S. Wan and Y. Wang, *Chinese J. Catal.*, 2019, **40**, 1810–1819.
- S6 C. Tao, A. Lv, N. Zhao, S. Yang, X. Liu, J. Zhou, W. Liu and J. Zhao, *Synlett*, 2011, 134–138.
- S7 (a) J. T. Scanlon and D. E. Willis, *J. Chromatographic Sci.*, 1985, **23**, 333–340; (b) T. Holm, *J. Chromatography A*, 1999, **842**, 221–227.
- S8 AIST: National Institute of Advanced Industrial Science and Technology (Japan), URL: https://sdbs.db.aist.go.jp/sdbs/cgi-bin/direct_frame_top.cgi
- S9 F. Ke, Y. Qu, Z. Jiang, Z. Li, D. Wu and X. Zhou, *Org. Lett.*, 2011, **13**, 454–457.
- S10 M. Kuhn, F. C. Falk and J. Paradies, *Org. Lett.*, 2011, **13**, 4100–4103.
- S11 WSS: Wiley Subscription Services, Inc. (US), URL: <https://sciencesolutions.wiley.com/>
- S12 M. Shimizu, T. Shimazaki and T. Konakahara, *Heterocycles*, 2010, **81**, 413–420.

NMR Spectra









JEOL RESONANCE

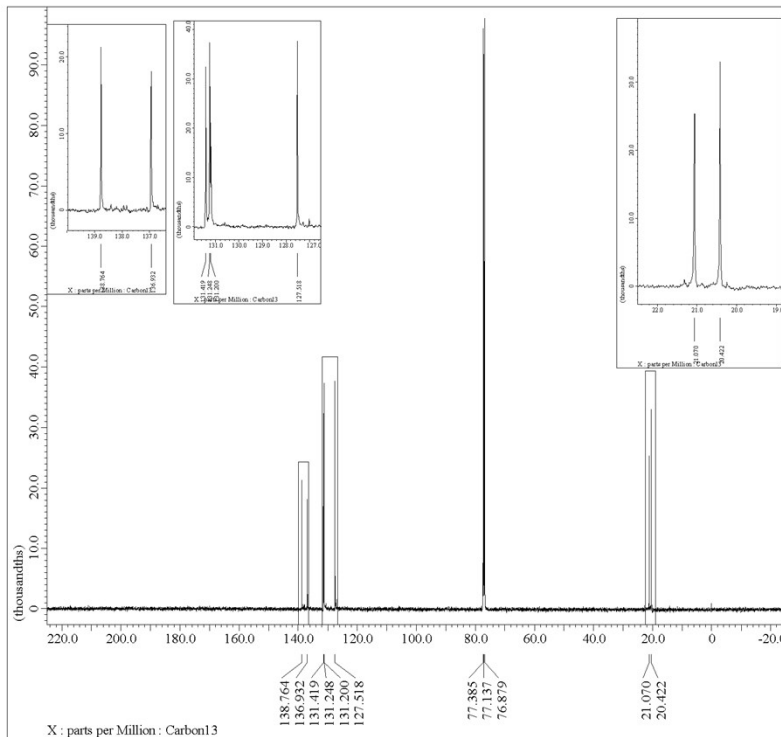
---- PROCESSING PARAMETERS ----
 dc balance (0, FALSE)
 seXP (0.2 [Hz], 0.0 [s])
 trapezoid (0 [s], 0 [s], 80 [s], 100 [s])
 zerofill (1)
 fft (1, TRUE, TRUE)
 machinephase
 ppm
 reference (0.02416 [ppm], 0 [ppm])

Filename = 200917_513_200917_513_1
 Author = delta
 Experiment = single_pulse.jxp
 Sample_id = 200917/513
 Solvent = CHLOROFORM-D
 Creation_Time = 17-DEC-2020 10:52:09
 Revision_Time = 23-DEC-2020 10:43:46
 Current_Time = 23-DEC-2020 10:44:11

Comment = single_pulse
 Data_Format = ID_COMPLEX
 Dim_Size = 26214
 Dim_Title = Proton
 Dim_Units = [ppm]
 Dimensions = X
 Site = JNM-ECA500
 Spectrometer = DELTA2_MMR

Field_strength = 11.7473579 [T] (500 [MHz])
 X_Acq_Duration = 3.4917580 [s]
 X_Domain = 1H
 X_Freq = 500.15991521 [MHz]
 X_Offset = 5.0 [ppm]
 X_Points = 32768
 X_Prescans = 1
 X_Resolution = 0.28638868 [Hz]
 X_Sweep = 9.38438458 [kHz]
 X_Sweep_Clipped = 7.50750751 [kHz]
 Irr_Domain = Proton
 Irr_Freq = 500.15991521 [MHz]
 Irr_Offset = 5.0 [ppm]
 Tr1_Domain = Proton
 Tr1_Freq = 500.15991521 [MHz]
 Tr1_Offset = 5.0 [ppm]
 Clipped = FALSE
 Scans = 8
 Total_scans = 8

Relaxation_Delay = 7 [s]
 Recvr_gain = 30
 Temp_Set = 22.9 [dC]
 X_90_Width = 11.12 [us]
 X_Acq_Time = 3.4917580 [s]
 X_Angle = 45 [deg]
 X_Atn = 2 [dB]
 X_Pulse = 5.54 [us]
 Irr_Mode = off
 Tr1_Mode = off



JEOL RESONANCE

---- PROCESSING PARAMETERS ----
 dc balance (0, FALSE)
 seXP (2.0 [Hz], 0.0 [s])
 trapezoid (0 [s], 0 [s], 80 [s], 100 [s])
 zerofill (1)
 fft (1, TRUE, TRUE)
 machinephase
 ppm

Filename = 200917_513_200917_513_13C-
 Author = delta
 Experiment = single_pulse_dec.jxp
 Sample_id = 200917/513
 Solvent = CHLOROFORM-D
 Creation_Time = 17-DEC-2020 10:57:39
 Revision_Time = 16-NOV-2020 11:59:03
 Current_Time = 16-NOV-2020 11:59:12

Comment = single_pulse_decoupled_gat
 Data_Format = ID_COMPLEX
 Dim_Size = 26214
 Dim_Title = Carbon13
 Dim_Units = [ppm]
 Dimensions = X
 Site = JNM-ECA500
 Spectrometer = DELTA2_MMR

Field_strength = 11.7473579 [T] (500 [MHz])
 X_Acq_Duration = 0.83361792 [s]
 X_Domain = 13C
 X_Freq = 125.76529768 [MHz]
 X_Offset = 100 [ppm]
 X_Points = 32768
 X_Prescans = 4
 X_Resolution = 1.19959034 [Hz]
 X_Sweep = 39.3081761 [kHz]
 X_Sweep_Clipped = 21.4454098 [kHz]
 Irr_Domain = Proton
 Irr_Freq = 500.15991521 [MHz]
 Irr_Offset = TRUE
 Clipped = TRUE
 Total_scans = 500

Relaxation_Delay = 8.3 [s]
 Recvr_gain = 32
 Temp_Set = 23.5 [dC]
 X_90_Width = 4.8 [us]
 X_Acq_Time = 0.83361792 [s]
 X_Angle = 30 [deg]
 X_Atn = 5 [dB]
 X_Pulse = 1.53333333 [us]
 Irr_Atn_Dec = 20.354 [dB]
 Irr_Atn_Rec = 20.354 [dB]
 Irr_Boise = WALTZ
 Irr_Pwidth = 92 [us]
 Decoupling = TRUE

